SANDIA REPORT
SAND2007-5882
Unlimited Release
Printed September 2007

Secure Portal

Cynthia L. Nelson

Prepared by
Sandia National Laboratories
Albuquerque, New Mexico 87185 and Livermore, California 94550

Sandia is a multiprogram laboratory operated by Sandia Corporation,
a Lockheed Martin Company, for the United States Department of Energy's
National Nuclear Security Administration under Contract DE-AC04-94AL85000.

Issued by Sandia National Laboratories, operated for the United States Department of Energy by Sandia Corporation.

Available to DOE and DOE contractors from
U.S. Department of Energy
Office of Scientific and Technical Information
P.O. Box 62
Oak Ridge, TN 37831

Telephone: (865) 576-8401
Facsimile: (865) 576-5728
E-Mail: reports@adonis.osti.gov
Online ordering: http://www.osti.gov/bridge

Available to the public from
U.S. Department of Commerce
National Technical Information Service
5285 Port Royal Rd.
Springfield, VA 22161

Telephone: (800) 553-6847
Facsimile: (703) 605-6900
E-Mail: orders@ntis.fedworld.gov
Online order: http://www.ntis.gov/help/ordermethods.asp?loc=7-4-0#online

SAND2007-5882
Unlimited Release
Printed September 2007

Secure Portal

Cynthia L. Nelson
Security Systems and Technology Center
Sandia National Laboratories
P.O. Box 5800
Albuquerque, NM 87185-0780

Abstract

There is a need in security systems to rapidly and accurately grant access of authorized personnel to a secure facility while denying access to unauthorized personnel. In many cases this role is filled by security personnel, which can be very costly. Systems that can perform this role autonomously without sacrificing accuracy or speed of throughput are very appealing. To address the issue of autonomous facility access through the use of technology, the idea of a "secure portal" is introduced. A secure portal is a defined zone where state-of-the-art technology can be implemented to grant secure area access or to allow special privileges for an individual. Biometric technologies are of interest because they are generally more difficult to defeat than technologies such as badge swipe and keypad entry. The biometric technologies selected for this concept were facial and gait recognition. They were chosen since they require less user cooperation than other biometrics such as fingerprint, iris, and hand geometry and because they have the most potential for flexibility in deployment.

The secure portal concept could be implemented within the boundaries of an entry area to a facility. As a person is approaching a badge and/or PIN portal, face and gait information can be gathered and processed. The biometric information could be fused for verification against the information that is gathered from the badge. This paper discusses a facial recognition technology that was developed for the purposes of providing high verification probabilities with low false alarm rates, which would be required of an autonomous entry control system. In particular, a 3-D facial recognition approach using Fisher Linear Discriminant Analysis is described. Gait recognition technology, based on Hidden Markov Models has been explored, but those results are not included in this paper. Fusion approaches for combining the results of the biometrics would be the next step in realizing the secure portal concept.

Acknowledgement

All facial recognition work for this project was performed by Trina D. Russ. Trina resigned from Sandia National Laboratories to pursue further 3-D facial recognition opportunities with Digital Signal Corporation.

Secure Portal

1. Introduction

Autonomous facility access could be realized through the concept of a "secure portal." A secure portal is a defined zone where state-of-the-art technology is implemented to grant secure area access or privileges. One of the technologies that would facilitate this idea is automatic facial recognition. Facial recognition is a promising technology for many applications because of its non-intrusive nature, ease of integration into existing systems, and potential to identify individuals at a distance without subject cooperation. These attributes make it ideal for the screening of individuals at borders, airports, secure facilities, etc. However, designing systems ideal for these environments requires systems that are robust to variations in facial pose, illumination, and expression. While the utilization of 3D data is an opportune choice to mitigate issues associated with illumination and pose variations, 3D data is still highly affected by variations in facial expression due to non-rigid facial deformations.

Among the unsupervised statistical learning techniques, Principle Component Analysis (PCA) and Linear Discriminant Analysis (LDA) are in the forefront, noted for their potential for dimensionality reduction and data generalization. PCA seeks to minimize the L2 norm between a PCA synthesized representation and an original signal, making it a good choice when a lower dimensional model of a signal class typically containing little within-class variation is desired. However, when the within-class variation is significant PCA can be less than optimal for a recognition task because within-class variations may be as or more significant than between-class variations causing great difficulty in the determination of highly accurate match decisions. LDA addresses this issue by determining a data basis from the training data that maximizes the between-class variations, while minimizing within-class variations. LDA and/or its variants have been applied to the 2D face recognition problem and have demonstrated significant improvement when presented with variations in illumination and expression [1, 2].

Despite the above, the generalization/overfitting problem with many of these systems is of major concern. In [1], Zhao *et al.* state that projecting data onto a lower-dimensional basis prior to applying LDA (subspace LDA) greatly improves this overfitting issue over standard LDA, especially when using very few training images per subject. However, Martinez and Kak [3] state that in applying even subspace LDA it is very important that the training samples are representative and uniformly sample the distribution for each class. In addition, if this is not the case then one may encounter situations where PCA outperforms LDA, thus, negating the entire motivation for using the approach.

This paper presents an approach for 3D face recognition using Fisher Linear Discriminant Analysis (FLDA) that demonstrates good recognition performance when provided with expression varying facial data. The robustness of the approach is in the deformation model used to align faces prior to projection onto a lower dimensional subspace; and in the power of using a class specific method (LDA) for recognition. In the formulation, when a semi-representative training set is used, good generalization performance is realized, and the performance is substantially better than PCA, given the same test and training sets.

The remainder of this paper is organized as follows. Section 2 summarizes related work in the area of 3D face recognition and in particular the use of PCA based approaches for recognition. In Section 3, a novel deformation model is discussed which provides the correspondences needed for PCA and LDA. Then, FLDA will be discussed in section 4 providing the framework for the presented recognition system. Finally, results of the system are presented in section 5.

2. Related Work

Since the launch of the FRGC, numerous approaches for the 3D and 2D+3D face recognition problems have emerged. The FRGC sought to motivate an order of magnitude improvement in face recognition technology by providing the research community with a standard set of data for analysis and associated challenge experiments [4]. Review articles of 3D based face recognition systems are provided in [5] and [6].

The FRGC v2 database contains variations in facial expression that were challenging for many algorithms. For instance, the FRGC baseline's Iterative Closest Point (ICP) and PCA algorithm's rank one identification rate dropped from 91% and 77% to 61.5% and 61.3% for neutral and non-neutral expressions, respectively. Some researchers have proposed to analyze expression insensitive regions to mitigate this problem. For example, Chang *et al.* [7] consider ICP based face matching with several probe surfaces concentrated around the nose elevating the rank one identification rate to 87% for expression varying data. However, Mian *et al.* [8] consider ICP base

matching using a nose and forehead region and achieve a 95.63% probability of detection (Pd) at .001 FAR using a neutral gallery set. Although, [8] reports improved results over [7] using a similar technique, one must realize that the probe images were only matched to neutral gallery images. The inclusion of non-neutral probe to non-neutral gallery matches would likely decrease performance. Nevertheless, [8] still performed better than [7] for neutral images indicating that the inclusion of the forehead region may add additional discrimination. This presents the issue that although removing face regions appears to benefit recognition with expression varying data, it may also remove some important information beneficial for recognition.

Other approaches have obtained good results in the presence of facial expressions while considering the whole face, outperforming the region based techniques. For instance, Kakadiaris *et al.* [9] present an annotated face model for recognition that deforms a reference face to an input face. The deformation information is subsequently encoded with wavelets and used for recognition. A Pd of 97.3% was obtained at .001 FAR. Log-Gabor wavelets were applied to the 3D face recognition problem in [10] achieving a 92.3% Pd at .001 FAR. Maurer *et al.* [11] present an approach that analyzes the distribution of errors after registering two faces with ICP. Integrating 3D and texture, they achieved a 92.8% Pd at .001 FAR. And, Husken *et al.* [12] integrate shape and texture information using a technique based on Hierarchical Graph Matching (HGM's) obtaining a 97.3% Pd at .001 FAR. To obtain a robust solution to the facial recognition problem it is important that the best performance is achieved in each modality. However, the performance of [11] and [12] drops to 87% and 89.5% respectively when only 3D information is used indicating the potential for improvement.. However, [9] is only based on 3D and thus, has the best reported 3D solution.

Even though LDA based techniques have been often applied to overcome some of the within-class variations apparent in 2D imagery [13], no results have been reported of using this approach directly to mitigate the 3D face expression problem. And although several PCA techniques have been applied to 3D face recognition [14] [15] [16].[17], these systems have typically fallen below the FRGC top performers. The exception may be [15] whose system was validated using only 60 subjects from an non-FRGC database. One thing to note is that many of these PCA approaches use a range-based (2.5D) representation. The exception is Russ *et al.* [14] who encode the x, y, and z components with PCA yielding a 95% Pd at .001 FAR when matching neutral probes to a single subject neutral gallery set.

Although, [9] has achieved good performance for expression varying data using only 3D data, it is believed that model based approaches such as PCA and LDA bring a unique perspective to the recognition problem and may be optimal in environments where the authorized user set is known. Therefore, this work builds upon [14] and analyzes the performance of LDA for expression varying data. It is believed that LDA/PCA approaches can be as or more accurate that 3D point matching schemes such as ICP if the 3D correspondence problem is properly addressed.

3. 3D Point Correspondence/Alignment

The correspondence calculation is a critical component of unsupervised statistical learning algorithms such as PCA, LDA, etc. and will impact the accuracy of the synthesized representation, the amount of data compression achievable, and furthermore recognition.

Only a few methods have been reported where 3D corresponded face coordinates are encoded with PCA. In [18], shape and texture correspondences for PCA were obtained by optical flow registration to a reference face. However, the 3D model was used to address the problem of pose variation for 2D face recognition systems. Also in [14] each input face was first iteratively aligned to a scaled reference face using ICP and subsequently deformed to approximate an input face using a surface normal correspondence procedure. While this deformation worked reasonably well, it can produce erroneous correspondences in surface regions that vary significantly from the input surface in distance or complexity.

The presented method for correspondences builds upon the approach in [14] and mitigates the associated correspondence issues. Addressing these correspondence issues for data containing variations in facial expression is of particular importance because of the significant differences that occur between drastic facial expressions and the neutral reference face used for correspondence. Thus, in this work the normal based deformation procedure is performed iteratively and more gradually than in [14] to better approximate the input surface.

A system diagram of the correspondence procedure is provided in Figure 1 with the deformation algorithm shown in the gray box outlined in black. At each iteration t of the deformation process the algorithm takes as inputs the registered input surface F, the current reference R_t and two parameters β and α that control the speed of deformation and smoothness of the deformed surface respectively. The output P_t is the current deformed

approximation to the input surface F and can be considered the corresponded surface upon completion (i.e. the result of correspondence between an input surface and a reference).

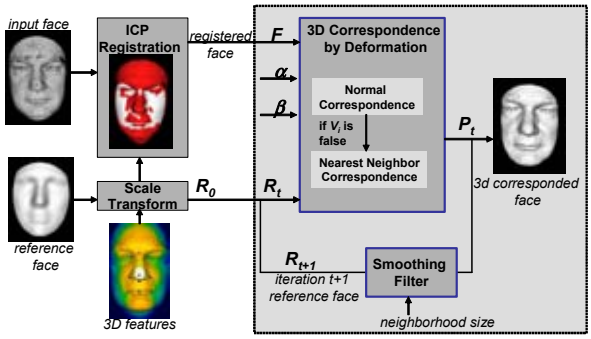

Figure 1. A system diagram of the correspondence procedure achieved by deforming a reference face.

The mathematical formulation of the deformation process is as follows. Consider a reference face R_t containing M 3D points that are updated at each time step to better approximate a constant input probe surface F.

$$P_{t,i} = \begin{cases} \alpha R_{t,i} + (1-\alpha) Q_i & if\ Q_i \neq \phi \\ \beta R_{t,i} + (1-\beta) W_{t,i} & else \end{cases} \qquad (3.1)$$

An approximation P_t to input surface F is achieved at each time step by determining a corresponding point on the input surface $W_{i,t}$ for each point i on the reference surface. The approximate surface P_t is defined by (3.1). In (3.1), α is in [0, 1] and controls the smoothness of the resulting representation versus maintaining the integrity of the input surface. Similarly, β, in [0, 1], controls the strength of the reference surface attraction towards the input surface and thus controls the magnitude of the pull towards surface F at teach time step. The term $W_{i,t}$ is the best corresponding point to reference point i at time t. This value is determined by either using the point at which the reference's normal vector ($N_{t,i}$) intersects the input surface F or by selecting the closest point on F to the current reference point. The normal surface intersection is the primary method for correspondences and is only abandoned if the normal vector is not long enough to intersect the input surface or if the point at which the normal vector intersects the surface is too far from a point actually on the surface. This condition is represented by the boolean V_i. In determining the normal intersection point, the length of the normal vector ($\Delta^r_{t,i}$) at reference point i is bounded by Δ^r_{MAX} and dynamically based on the current reference to input surface distance. If a valid normal vector surface intersection, represented by the boolean V_i, cannot be found, the closest point to the input surface is used as shown in (3.2).

Each time step brings the reference surface closer to the input surface F. When the distance between the reference surface and $W_{t,i}$ is less than some tolerance Δ^r_{TOL}, a point Q_i is defined as the final correspondence between the reference face at point i and the input surface F. Once Q_i is defined, the correspondence search for point i is not conducted at future time steps. This enables the process to terminate when all the Q_i's have been defined.

$$W_{t,i} = \begin{cases} R_{t,i} + \Delta^r_{t,i} N_{t,i} & if\ V_i = true \\ \min \left\| R_{t,i} - F \right\| & else \end{cases} \qquad (3.2)$$

At each time step, the reference face is updated by convolving P_t with a smoothing filter H. This helps to ensure that the reference surface is smooth and contains well conditioned surface normals.

$$R_{t+1} = P_t * H \qquad (3.3)$$

This approach seeks to minimize the error function E_t defined as the cumulative distance between the current reference R_t and the approximate surface P_t shown in (3.4). The described deformation process is iteratively performed until E_t or $|E_t - E_{t-1}|$ is less than some tolerance, all Q_i's have been defined, or K iterations have been performed.

For this work a statistical mean of faces was used as the initial reference face, shown in Figure 2. Prior to deformation, each input face F is segmented, filtered to remove noise and fill holes, and registered to a scaled version of the reference face using ICP. The reference face was scaled vertically as in [14] using sellion and mouth features that were autonomously detected using radial symmetry [19]. Examples of segmented faces and their resulting deformed faces are shown in Figure 3 for various facial expressions of the same subject.

$$E_t = \sum_{i=1}^{M} \left\| P_{t,i} - R_{t,i} \right\| \qquad (3.4)$$

Figure 2. The Initial 3D Reference Face (R_0)

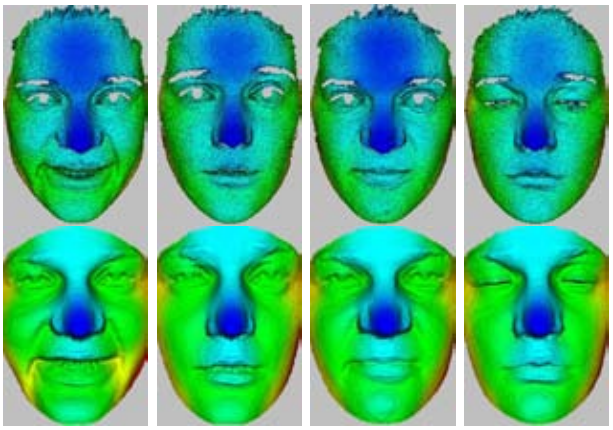

Figure 3. 3D Point Correspondence by Reference Deformation. Top) The segmented, but unregistered input surface. Bottom) The approximate input surface P_t achieved by reference surface deformation. Each column corresponds to a different acqusition of the same subject. Each surface is colored by its z coordinate where blue is the closest to the camera and red is the farthest.

It is important to note that this simplified formulation of the deformation process can be used because holistic scale changes in the deformation process do not have to be accounted for since the initial reference face R_0 was scaled prior to facilitate ICP registration.

This approach is similar to deformable models [20] in the sense that there are external forces towards which the model is pulled and internal smoothness constraints that regularize the resulting model. However, this approach typically converges in a few iterations and allows greater control over the deformation process by guiding the direction and rate of the reference surface attraction to an input surface.

4. Fisher Linear Discriminant Analysis

The formulation of the FLDA presented here is based on the fisherface method of [2]. Fisher Linear Discriminant Analysis selects a basis W such than the ratio of the between-class scatter S_B to the within-class scatter S_W is maximized as shown in (4.1).

$$W_{opt} = \max_{W} \frac{\left| W^T S_B W \right|}{\left| W^T S_W W \right|} \qquad (4.1)$$

Consider a set of N training samples containing C classes and N_i samples for each class i represented by the set X_i.

Given this, the between-class scatter matrix is computed by (4.2) where μ_i is the mean of each class in the training samples and μ is the mean over all training samples. The within-class scatter matrix is defined by (4.3) where x_k is the *k*th sample in class *i*.

$$S_B = \sum_{i=1}^{C} N_i (\mu_i - \mu)(\mu_i - \mu)^T \qquad (4.2)$$

$$S_W = \sum_{i=1}^{C} \sum_{x_k \in X_i} (x_k - \mu_i)(x_k - \mu_i)^T \qquad (4.3)$$

$$S_B w_i = \lambda_i S_W w_i \qquad (4.4)$$

The optimal solution to (4.1) can be posed as the generalized eigenvalue problem shown in (4.4). If S_W is nonsingular, W can be solved using $S_W^{-1} S_B$, however, the rank of S_W is at most $N - C$. Thus, in practice a non-singular S_W is difficult to achieve because the dimension of each sample x_k (H) is often much greater than the number of training examples (N). This is referred to as the curse of dimensionality.

Projecting training samples onto a lower-dimensional subspace can address a number of issues associated with the traditional formulation of FLDA. First, a nonsingular within scatter matrix can be obtained by carefully choosing the dimension M of the subspace. Second, the *overfitting/generalization* problem is improved [1]. And third, the space complexity is greatly reduced through the examination of *MxM* scatter matrices opposed to *HxH*. To obtain some of these benefits training samples were first projected onto a PCA basis of dimension M. Since PCA already requires a mean subtracted signal before projection, the mean training sample μ becomes zero in (4.2).

While a non-singular S_W is attractive for computational reasons, it is important that this is not the driving force for the selection of the basis size M, since this can significantly impact recognition performance. Therefore the generalized eigenvalue problem is solved in a way that can accommodate a singular S_W. There are several formulations of the generalized eigenvalue problem. The approach used here is based on the utilization of the QZ algorithm [21], for it appears to be more robust, yielding higher recognition results, than when using the inverse of a nonsingular S_W.

For 3D face recognition, the difference between a registered and corresponded 3D face and reference is encoded with the described subspace methods. The data vector x_k contains a list of 3d coordinates $(\Delta x_i, \Delta y_i, \Delta z_i)$ representing the variation of the input surface from the reference surface at point *i*. Figure 4 presents the first three basis vectors for PCA and FLDA respectively. To improve visualization, a single basis vector is represented by three images generated by using the corresponding $\Delta x_i, \Delta y_i,$ and Δz_i vectors to color the reference surface. Notice how the *z* component of the PCA basis vectors appears to isolate face changes to different regions of the face. For example, the *z* component PCA basis vectors 1, 2, and 3 are isolated to the nose, mouth, and cheeks respectively. The FLDA basis vectors although different, look more random; discernible facial features are difficult to see.

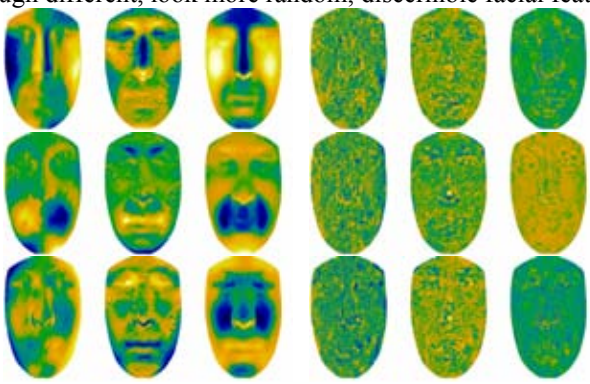

a) PCA Basis Vectors b)FLDA Basis Vectors

Figure 4. The X, Y, and Z components of the first 3 vectors from the (a) PCA Basis and (b) FLDA Basis

5. Experimental Results

5.1. Database Description

Analysis of the presented system is performed for 3D facial verification using databases from the Facial Recognition Grand Challenge database versions 1 and 2 (FRGC v1 and v2) [4].

The 3D images were acquired with the Minolta Vivid 900/910 range scanner and contain a 640x480 array of 3D points and a registered 640x480 color image. The color image is not used for the algorithm presented in this paper.

FRGC v1 consists of images of 275 subjects acquired in the spring of 2003 resulting in 943 images. The FRGC v2 database was acquired during the fall of 2003 and spring of 2004 and contains significant variations in facial expressions. This FRGC v2 dataset contains 466 subjects and 4007 images of which 1643 contain non-neutral expressions. Examples of expression variation are shown in Figure 3.

5.2. Subspace Training

A training set for PCA and FLDA was extracted from the combined FRGC v1 and v2 database. In creating this set, it is important to have both a good sampling of faces and a good sampling of face expressions. However, it is not necessary for each expression to be present for each subject, although, this will likely improve the overall results. For this database, expressions were partitioned into six groups: astonished, disgusted, frowning, sad, smiling, puffy, and neutral. For each expression class, a gallery was created containing the first occurrence of each subject in each expression class. These gallery sets were then combined to form 1927 images from which to derive the training set. In the following experiments, 250 subjects and their associated images (828) from this set were used for PCA and FLDA training. The number of training images compared to the number of test images used for each subject is shown in Figure 5.

Figure 5. Distribution of Training and Testing Samples Per Subject

5.3. Face Recognition

The match metric used for facial recognition is the cosine of the angles between the subspace coefficients [22]. Z-norm gallery score normalization as described in [23] was performed for both PCA and FLDA face recognition. Normalization seems to be beneficial on large datasets where there is significant variation associated with the within-class data samples such as expression.

PCA Recognition

To establish a baseline for performance, results using PCA coefficients as features for recognition are first presented. Face matching was performed using the combined FRGC v1 and v2 database resulting in 4950x4950 matches. For the PCA results, whitening was performed during matching. Face samples were projected onto the entire PCA basis of dimension M=827 (defined by the number of training samples minus one). However, only 25% of the coefficients were used for matching (approximately 200). We found that using all of the coefficients resulted in an overfitting of the subjects used in training, whereby, recognition of subjects included in training was worse than the recognition of untrained subjects. The trailing PCA coefficients were then removed to minimize this issue and improve overall performance. The Receiver Operating Character (ROC) curve representing the verification rate versus the false alarm rate is shown in Figure 6. The overall Pd at .001 FAR is 85.08%. Note that, using all of the

coefficients for matching resulted in a verification rate of 77%. As expected, good recognition performance is obtained for neutral faces (97.55% at .001 FAR), while a considerable performance decrease is observed for expressions (58.55% at .001 FAR). In the following section, the benefit of using FLDA for this problem is demonstrated.

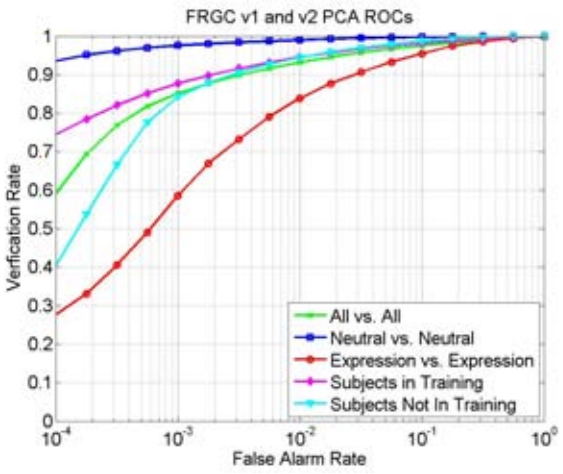

Figure 6. PCA 3D Face Recognition ROCs.

FLDA Recognition

Since only 250 training samples are used, the resulting dimension of the FLDA basis is at most *C-1* resulting in 249 features for our experiments. During matching no whitening or scaling is conducted in either PCA or FLDA space. The resulting FLDA ROC's are shown in Figure 7. Notice that FLDA has improved recognition performance for the neutral and non-neutral categories, achieving 98.7% and 95.8% Pds at .001 FAR for these categories respectively. FRGC v2 ROC's are shown for comparison to other 3D face recognition algorithms that use this database and are approaching the best reported results using this database [9]. The improvement over PCA amounts to approximately an increase in 37 percentage points at .001 FAR for non-neutral expressions. This demonstrates that FLDA is truly able to suppress the within-class variations thereby reducing the match score differential between within-class samples.

As stated in section 3, the training sample data is first projected onto a lower dimension PCA basis prior to performing FLDA. The size of the selected PCA dimension is 100% of the full PCA space defined by the number of training samples minus one (*N-1*). Although this resulted in a singular S_W, it consistently performed better than pruning the PCA basis to $M <= N-C$ to obtain a non-singular S_W. We attribute this to the fact that in order for FLDA to properly maximize between-class variations while minimizing within-class variations, these variations should be properly represented in the data. In [1], removing trailing basis vectors was justified by the argument that they represent noise and removing them will lead to greater generalization. However, in the presented system trailing basis vectors may correspond to real expression features and furthermore, if noise is a typical component of the data to be analyzed by the system, these are variations that LDA can learn to be robust against. This may explain the higher performance of FLDA on neutral faces than PCA. It is important to note that the method selected to solve the general eigenvalue problem can also have a significant impact on recognition performance. MATLAB's eigensolver, which uses the QZ algorithm, has been found to be robust and stable.

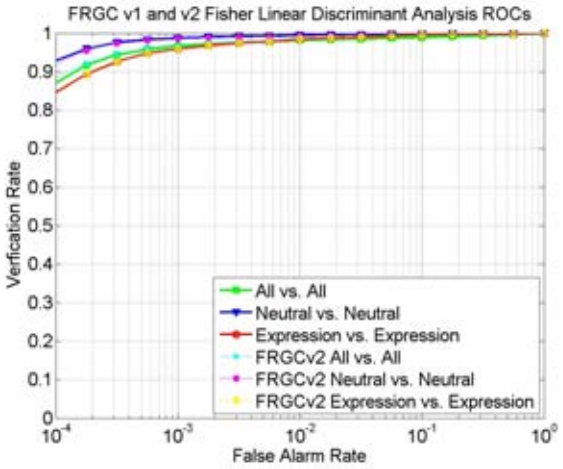

Figure 7. FLDA 3D Face Recognition ROCs.

5.4 FLDA Generalization

Although, FLDA appears to be an extremely promising approach for addressing the facial expression problem, one must remember that it is a class specific unsupervised learning algorithm, thus, it is important to understand how it performs with respect to the overfitting/generalization problem.

For this reason, the combined FRGC v1 and v2 database was partitioned into two sets referred to as dependent and independent. The dependent set contains subjects that were included in the training set, while the independent sets contains subjects that were not. This partition resulted in 2665 and 2284 dependent and independent samples respectively. The ROC curves for these sets appear in Figure 8. These curves demonstrate that the system performs extremely well on trained subjects, even with numerous untrained expressions per subject (99.1% at .001 FAR). Compared to the dependent set, there is a noticeable performance decrease for the independent set. However, the approach still demonstrates a good ability to learn untrained subjects and their associated expressions (95% at .001 FAR). It is interesting to note that the dependent set of samples performed slightly better than the neutral samples, indicating that FLDA is fully capable of accommodating expressions, but could benefit from improvement in generalizing these learned expressions to the expressions of new subjects.

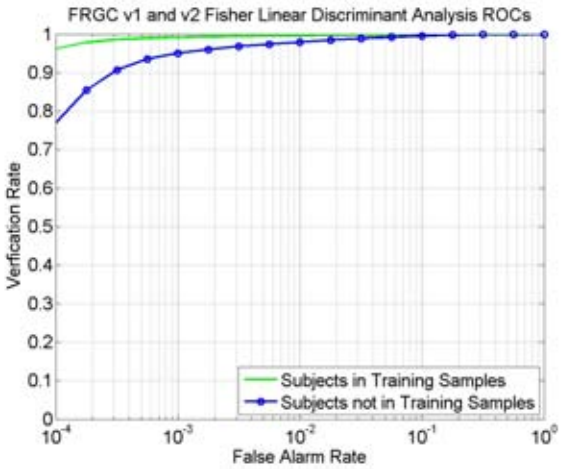

Figure 8. FLDA 3D Face Recognition ROCs Representing the Generalization Issue

6. Conclusion

Although, FLDA is known for dealing with within-class variations, this paper includes the first reported results of using the method to accurately solve the facial expression problem in 3D. The presented FLDA approach provides a dramatic improvement over using PCA for the same database. We also believe the iterative registration and deformation processes used to obtain good correspondences are instrumental in achieving the results presented. The accuracy of this stage enables good generalization to new untrained subjects.

A summary of results obtained using the FLDA approach is presented in Table 1. Given these results, the presented approach would be competitive with the best reported FRGC 3D performer [9] whose highest reported results are 97.3% Pd at .001 FAR (95.6% and 99.0% for non-neutral and neutral expressions respectively). While [9] has achieved higher performance overall, we believe we have higher accuracy potential for known subjects where training samples can be obtained (i.e. 99.1%). The FLDA 3D face recognition approach is ideal for access control environments where the authorized users are known. In this setting, samples of subjects and their expression variations can be obtained resulting in a system that is extremely accurate.

Table 1. Summary of FLDA 3D Face Recognition Results

FLDA Description	**Verification Rate At .001 FAR**
All vs. All	96.6%
Neutral vs. Neutral	98.7%
Expression vs. Expression	95.8%
Dependent Subjects All vs. All	99.1%
Independent Subjects All vs. All	95.0%

In future efforts, the FLDA 3D face space will be further explored to determine its limit. For instance, at what point do adding new faces fail to improve generalization and potentially decrease performance for the known subjects? It has already been observed that increasing the training set size from 200 to 250 subjects increased the overall performance by several percentage points. At what point will this cease? In addition, it is of interest to fuse these 3D results with texture data to obtain additional robustness and accuracy.

References

[1] W. Zhao, R. Chellapa, and P. J. Phillips, "Subspace linear discriminant analysis for face recognition," University of Maryland, College Park CS-TR-4009, April 1999.

[2] P. Belhumeur, J. Hespanha, and D. Kriegman., "Eigenfaces vs. Fisherfaces: Recognition using class specific linear projection," *IEEE Transactions on Pattern Analysis and Machine Intelligence*, vol. 19, pp. 711-720, 1997.

[3] A. M. Martinez and A. C. Kak, "PCA versus LDA," *IEEE Transactions on Pattern Analysis and Machine Intelligence*, vol. 23, pp. 228-233, 2001.

[4] P. J. Phillips, P. J. Flynn, T. Scruggs, K. W. Bowyer, J. Chang, K. Hoffman, J. Marques, J. Min, and W. Worek", "Overview of the face recognition grand challenge," presented at Computer Vision and Pattern Recognition (CVPR), San Diego, CA, 2005.

[5] K. Chang, K. Bowyer, and P. Flynn, "An evaluation of multi-modal 2D+3D face biometrics," *IEEE Transactions on Pattern Analysis and Machine Intelligence*, vol. 27, pp. 619-624, 2005.

[6] R. Paquet and A. Z. Kouzani, "Advances in 3D-based face recognition," presented at International Joint Conference on Neural Networks, Vancourver, BC, Canada, 2006.

[7] K. I. Chang, K. W. Bowyer, and P. J. Flynn, "Multiple nose region matching for 3D face recognition under varying facial expression," *IEEE Transactions on Pattern Analysis and Machine Intelligence*, vol. 28, 2006.

[8] A. Mian, M. Bennamoun, and R. Owens, "Automatic 3D Face Detection, Normalization, and Recognition," presented at Third International Symposium on 3D Data Processing, Visualization and Transmission (3DPVT), 2006.

[9] I. Kakadiaris, G. Passalis, G. Toderici, N. Murtuza, and T. Theoharis, "3D Face Recognition," presented at BMCV: British Machine Vision Conference, Edinburgh, 2006.

[10] J. Cook, V. Chandran, and C. Fookes, "3D face recognition using log-gabor templates," presented at British Machine Machine Vision Conference, Edinburgh, 2006.

[11] T. Maurer, D. Guigonis, I. Maslov, B. Pesenti, A. Tsaregorodtsev, D. West, and G. Medioni, "Performance of Geometrix ActiveIDTM 3d face recognition engine on the FRGC data," *IEEE Workshop on Face Recognition Grand Challenge Experiments*, 2005.

[12] M. Husken, M. Brauckmann, S. Gehlen, and C. Malsburg, "Strategies and benefits of fusion of 2D and 3D face recognition," in *IEEE Workshop on Face Recognition Grand Challenge Experiments*, 2005.
[13] X. Lu, A. Jain, and D. Colbry, "Matching 2.5D face scans to 3D models," *IEEE Transactions on Pattern Analysis and Machine Intelligence*, vol. 28, pp. 31-43, 2006.
[14] T. Russ, C. Boehnen, and T. Peters, "3d face recognition using 3d alignment for PCA," in *IEEE Conference on Computer Vision and Pattern Recognition*. New York, New York, 2006.
[15] X. Yuan, J. Lu, and T. Yahagi, "A method of 3d face recognition based on principal component analysis algorithm," *IEEE Symposium on Circuits and Systems*, vol. 4, pp. 3211-14, 2005.
[16] C. Hesher, A. Srivastava, and G. Erlebacher, "A novel technique for face recognition using range imaging," in *Seventh International Symposium on Signal Processing and Its Applications*, 2003, pp. 201--204.
[17] C. McCool, V. Chandran, and S. Sridharan, "2D-3D hybrid face recognition based on PCA and feature modeling," presented at Second Workshop on Multimodal User Authentication Toulouse, France, 2006.
[18] V. Blanz and T. Vetter, "Face recognition based on fitting a 3d morphable model," *IEEE Transactions on Pattern Analysis and Machine Intelligence*, vol. 25, pp. 1063-1074, 2003.
[19] M. L. Koudelka, M. W. Koch, and T. D. Russ, "A prescreener for 3D face recognition using radial symmetry and the Hausdorff fraction," *IEEE Workshop on Face Recognition Grand Challenge Experiments*, 2005.
[20] M. Kass, A. Witkin, and D. Terzopoulos, "Snakes: active contour models," *International Journal of Computer Vision*, vol. 1, pp. 321-331, 1988.
[21] G. H. Golub and C. F. V. Loan, *Matrix Computations*, Third ed. Baltimore and London: The John Hopkins University Press, 1996.
[22] R. Beveridge, D. Bolme, M. Teixera, and B. Draper, "The CSU face identification evlaution system user's guide version 5.0," in *http://www.cs.colostate.edu/evalfacerec*.
[23] P. J. Phillips, D. M. Blackburn, J. M. Bone, P. Grother, R. J. Michaels, and E. Tabassi, "Face Recognition Vendor Test," in *www.frvt.org*, 2002.

Distribution

1	MS	0123	D. L. Chavez (LDRD Office), 1011
1	MS	0780	Stephen Ortiz, 6484
5	MS	0780	Cynthia L. Nelson, 6474
2	MS	9018	Central Technical Files, 8944
2	MS	0899	Technical Library, 9536